Communication

A Novel Wideband Tightly Coupled Dual-Polarized Reflectarray Antenna

Wenting Li, Hancheng Tu, Yejun He, Long Zhang, Sai-Wai Wong, and Steven Gao

***Abstract*— In this communication, a novel tightly coupled dual-polarized reflectarray antenna is presented. The antenna consists of a dual-polarized feed antenna and a wideband dual-polarized reflecting surface. The reflecting surface is composed of dual-polarized tightly coupled unit cells. Each unit cell contains two types of elements, of which the polarizations are perpendicular. Each element contains a dipole and a delay line. For one polarization, the reflecting surface consists of 13 × 34 elements, while there are 26 × 11 elements on the reflecting surface for the other polarization. The feed antenna is a wideband dual-polarized horn antenna. The phase error distribution on the reflecting surface is analyzed as well. To verify the design, a prototypical tightly coupled dual-polarized reflectarray antenna operating from 3 to 8 GHz is simulated, manufactured, and measured. The simulated results are in good agreement with the measured results. In the working band, the radiation patterns of the proposed reflectarray antenna are stable.**

***Index Terms*— Dual-polarized reflectarray, reflectarrays, tightly coupled reflectarrays, wideband reflectarrays.**

I. Introduction

Reflectarray antenna is an attractive hot topic at present which features low cost, compared with the parabolic reflector antenna. The reflectarray antenna also has a relatively simple feed network.

In [1], the patches with different shapes and sizes are used as the unit cell to construct the reflectarray antenna. In [2], the dipoles with different lengths are selected to design the reflectarray antenna. In [3], the slots with different lengths are applied to control the phase of the unit cell on the reflecting surface.

Although the reflectarray antenna has the advantages mentioned above, its bandwidth is usually not wide. Therefore, many researchers have tried to broaden the bandwidth of the reflectarray antenna. In [4] and [5], the dipoles are placed in parallel to enlarge the gain bandwidth of the reflectarray. In [6], the stacked patch elements are used to widen the bandwidth of the reflectarrays. In [7], the subwavelength elements are used to design the wideband reflectarray. In [8], [9], [10], and [11], the tightly coupled dipoles are employed to broaden the bandwidth of reflectarray antennas.

Although the bandwidth of the tightly coupled reflectarray antenna in [8] and [9] is enlarged a lot, it is a single-polarized reflectarray. However, to enlarge the communication capacity, multi-polarized wideband reflectarrays are needed. Some scholars study dual-polarized reflectarray antennas.

In [5], the element contains coplanar parallel dipoles to realize the dual-polarized reflectarray. In [12], the stacked crossed dipoles are applied to design the dual-polarized unit. In [13], the 1-bit reconfigurable unit is proposed to realize the dual-polarized waves. In [14], the broadband dual-polarized reflectarray is built based on the stacked Jerusalem crosses.

In this communication, a novel tightly coupled broadband dual-polarized reflectarray antenna is proposed. A dual-polarized unit cell containing two types of elements is designed to build the reflectarray antenna. Each element consists of a dipole and a delay line. In one unit cell, the numbers of the two types of elements are different. The method of calculating the numbers is given as well. A dual-polarized horn antenna is employed to provide the dual-polarized incident waves. Although a tightly coupled dual-polarized reflectarray antenna is reported in [10], it is not realized in practice and not measured.

The rest of this communication is organized as follows. The detailed design of the proposed reflectarray is shown in Section II. The simulated and measured results are shown in Section III. Section IV concludes the communication.

II. Design of the Tightly Coupled Dual-Polarized Reflectarray

In this section, a wideband tightly coupled dual-polarized reflectarray antenna working from 3 to 8 GHz is designed. Then, the phase error distribution on the reflectarray surface is discussed and its effect on the array factor of the reflectarray antenna is analyzed.

A. Dual-Polarized Unit Cell

In [8], a tightly coupled wideband reflectarray antenna is designed with a working band of 3.4–10.6 GHz, which is a single-polarized reflectarray antenna. Based on the unit cell in [8], a dual-polarized tightly coupled unit cell is proposed. The geometry of the proposed dual-polarized unit cell is shown in Fig. 1.

The proposed unit cell is printed on Rogers 4003C. Its permittivity and the loss tangent are 3.55 and 0.0027, respectively. The thickness of the substrate is 0.813 mm. Each unit cell consists of elements along the x- and y-axes. The elements along the x- and y-axes are called X and Y elements, respectively, which are shown in Fig. 1(b) and (c). Each element is composed of a dipole, a delay line, and two layers of ground. The dipole is attached to the top of the delay line. The delay line is a pair of parallel microstrips. In the operating band, the impedance of the delay line matches that of the dipole. For the delay line passing through the first ground, each element has a 4-mm diameter hole on the first ground. The distance from the top of the unit cell to the first ground is h_1, and the height from the first ground to the second ground is h_2. The shapes and sizes of the dipoles of X and Y elements are different. The width of the delay line of the

Manuscript received 25 May 2022; revised 17 February 2023; accepted 5 March 2023. Date of publication 3 April 2023; date of current version 2 June 2023. This work was supported in part by the National Natural Science Foundation of China under Grant 62101341 and Grant 62071306; and in part by the Shenzhen Science and Technology Program under Grant 20200810131855001, Grant JCYJ20200109113601723, Grant JSGG20210802154203011, and Grant JSGG20210420091805014. *(Corresponding author: Yejun He.)*

Wenting Li, Hancheng Tu, Yejun He, Long Zhang, and Sai-Wai Wong are with the State Key Laboratory of Radio Frequency Heterogeneous Integration, Guandong Engineering Research Center of Base Station Antennas and Propagation, Shenzhen Key Laboratory of Antennas and Propagation, College of Electronics and Information Engineering, Shenzhen University, Shenzhen 518060, China (e-mail: heyejun@126.com).

Steven Gao is with the Department of Electronic Engineering, The Chinese University of Hong Kong, Hong Kong, China.

Color versions of one or more figures in this communication are available at https://doi.org/10.1109/TAP.2023.3262969.

Digital Object Identifier 10.1109/TAP.2023.3262969

TABLE I
PARAMETERS OF THE REFLECTARRAY ELEMENT (UNIT: MM)

t_1	t_2	h_1	h_2	h_3	h_4	D	dx	dy	lf_1	lf_2	wx_1	wx_2	wx_3	wy_1	wy_2	wy_3
0.813	0.813	14.5	20	2.5	12	4	19.2	16	2	0.8	1.5	1	1	6	1	1.1

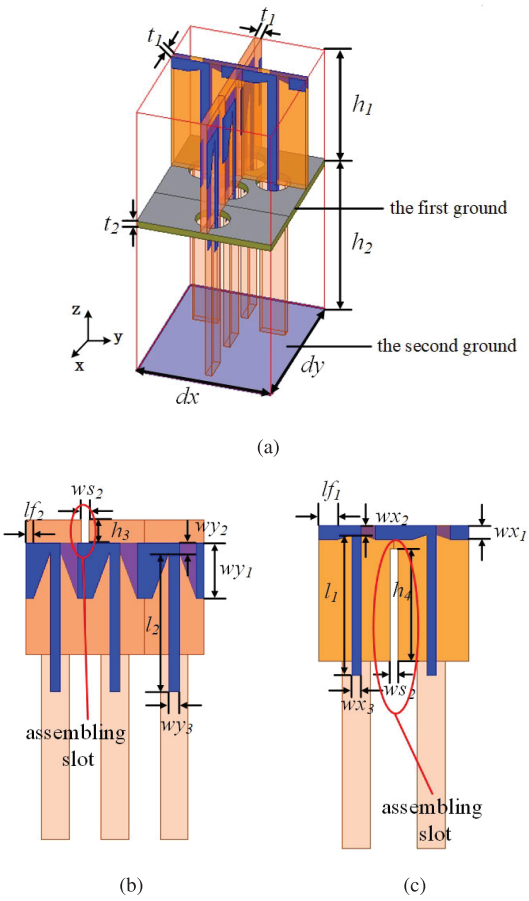

Fig. 1. (a) Geometry of the proposed unit cell, (b) front view of the X element, and (c) front view of the Y element.

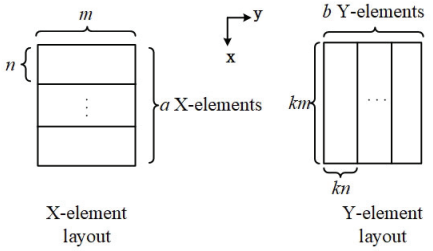

Fig. 2. Layout of the X and Y elements.

X element is wy_3, while that of the Y element is wx_3. The lengths of delay lines of X and Y elements are l_2 and l_1, respectively.

The next key question is to determine the numbers of the X and the Y elements in one unit cell and their dimensions. In one unit cell, it is assumed that there are a X and b Y elements. The layouts of X and Y elements in one unit cell are shown in Fig. 2. To guarantee the performance of the X element is similar to that of the Y element as much as possible, the size of the X element is set to be proportionate

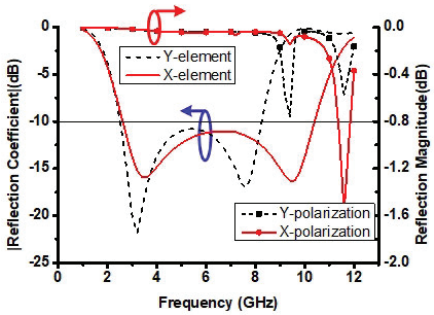

Fig. 3. Simulated reflection coefficients of the X and Y elements and reflection magnitude of the unit cell.

to that of the Y element. That is, if the size of the X element is $m \times n$, then that of the Y element is $kn \times km$. Therefore, equations can be given by:

$$a \cdot n = km \tag{1}$$

$$m = kn \cdot b. \tag{2}$$

Multiplying (1) and (2) together, then we obtain

$$a \cdot b = (m/n)^2. \tag{3}$$

From the previous work in [8], m/n is 2.5. So, $a{\cdot}b$ should be 6.25. Considering a and b are positive integers, the nearest $a{\cdot}b$ is 3×2 or 2×3. In the proposed design, $a = 3$ and $b = 2$. As a result, the size of the X element is $dx \times dy/3$ and that of the Y element is $dx/2 \times dy$. The parameters of the reflectarray element are shown in Table I. Considering the physical realizability of the unit cell, assembling slots are added at the intersection of the X and Y elements. The slots make it possible that the two types of elements can be assembled perpendicularly, as shown in Fig. 1.

The distance between the dipole and the first ground affects the impedance bandwidth of the element a lot. It can be seen that distance in the X element is smaller than that in the Y element. The distance difference is h_3. To avoid the X element touching the Y element and improve the isolation between them, h_3 is set to be larger than the width of the dipole in the Y element wx_1.

The impedance bandwidth of the X element is from 2.8 to 10.6 GHz, while that of the Y element is from 2.6 to 8.2 GHz, which are shown in Fig. 3. This is mainly due to the different sizes of the two types of elements and the existence of h_3. The reflection magnitude of the unit cell for X and Y polarization is higher than -0.2 dB from 2 to 9 GHz, which is shown in Fig. 3 as well.

The equivalent distance delay in [8], [15] is used to evaluate the proposed unit cell. The equivalent distance delay of the X and Y elements can provide is shown in Fig. 4. $d_f(l_2)$ is the curve of the equivalent distance delay of the X element with l_2 at the frequency f, while $d_f(l_1)$ is the curve of the equivalent distance delay of the Y element with l_1 at the frequency f. When l_1 or l_2 are fixed, the equivalent distance delay only varies slightly at different frequencies. For the two types of elements, the equivalent distance delay is convergent in the working band, which indicates that the proposed unit cell is with wideband performance.

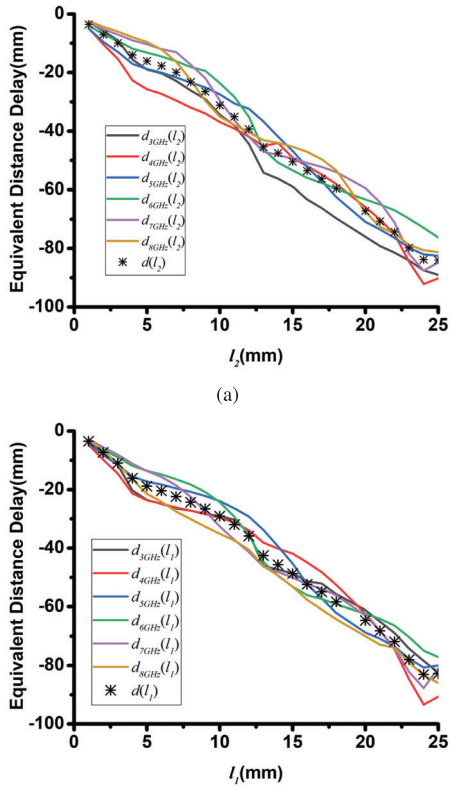

Fig. 4. Equivalent distance delay of the proposed (a) X and (b) Y elements.

TABLE II
PARAMETERS OF THE HORN ANTENNA (UNIT: MM)

l_3	h_5	h_6	h_7	t_3	t_4	d_2	wx_4
32.5	28	8	10	2	2	14.8	2.7
h_9	h_8	l_5	d_1	wy_4	h_{10}	l_6	
10.7	50	64	9.7	2.6	15.3	64	

To make the proposed element relatively stable for each frequency in the working band from f_1 to f_2, average curves $d(l_1)$ and $d(l_2)$ are employed to design the proposed dual-polarized reflectarray. $d(l_1)$ and $d(l_2)$ are calculated from (7) in [8, eq. (7)].

B. Dual-Polarized Feed Horn Antenna

In the proposed reflectarray, a dual-polarized horn antenna is chosen as the feed antenna. The horn antenna is manufactured based on 3-D printing.

Fig. 5 shows the configuration of the horn antenna. The parameters of the horn antenna are shown in Table II. The phase center of the horn antenna changes with different frequencies for both X- and Y-polarized waves, which is shown in Table III. The position of the phase center $p(z)$ applied in this design is calculated by [8, eq. (9)], which is -37.7 mm.

C. Reflectarray Design

The configuration of the reflectarray is shown in Fig. 6. The reflectarray is composed of a dual-polarized horn antenna and a dual-polarized reflecting surface, which includes 13 $\times$ 34 X elements and 26 $\times$ 11 Y elements. The size of the reflecting surface is 217.6 $\times$ 208 $\times$ 34.5 mm. The distance from the horn antenna to the reflecting surface Rh_1 is 110.5 mm and that from phase center to the reflecting surface Rh_2 is 148.2 mm.

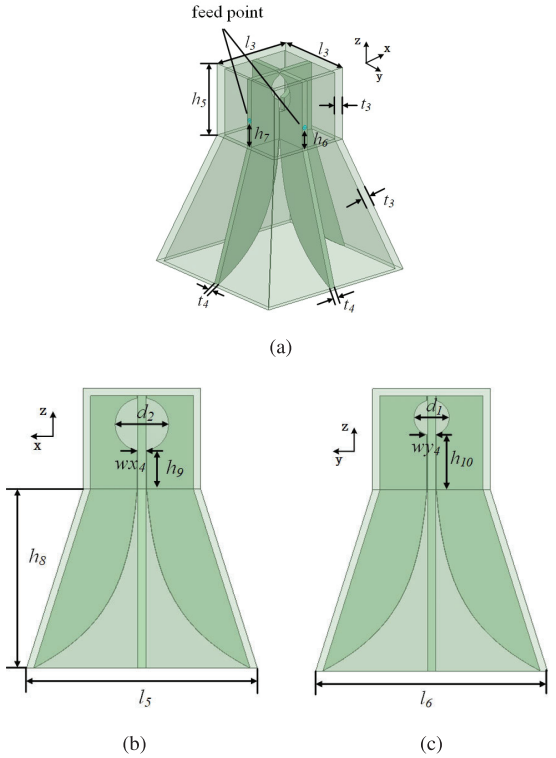

Fig. 5. Configuration of the dual-polarized feed horn antenna (a) 3D view, (b) front view, (c) side view.

TABLE III
COORDINATES OF PHASE CENTER (UNIT: MM)

Frequency (GHz)	3	4	5	6	7	8
$p_f(z)$ of x-polarized wave	-54	-46	-43	-37.6	-16.8	-29
$p_f(z)$ of y-polarized wave	-54	-46	-43	-37.5	-16.8	-29.1

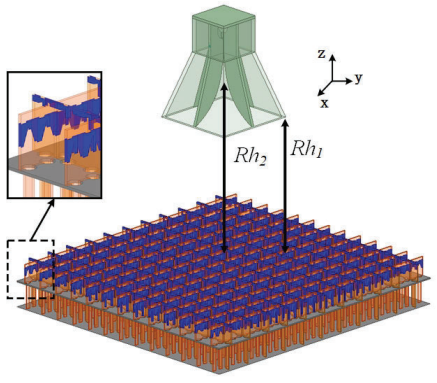

Fig. 6. Configuration of the proposed tightly coupled dual-polarized reflectarray antenna.

D. Phase Error Distribution and Its Effects on the Array Factors

Theoretically, after the electromagnetic wave is reflected by the reflecting surface, the phase of the reflected wave should be equal for

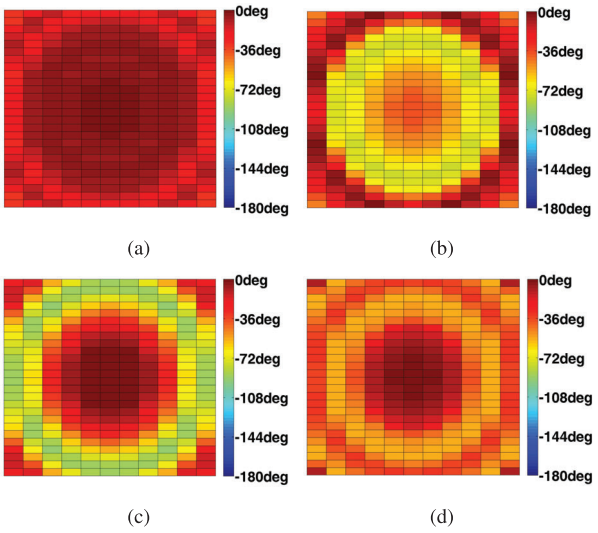

Fig. 7. Phase error distribution at (a) 3, (b) 5, (c) 6, and (d) 8 GHz when $d(l_2)$ is used to design the reflectarray.

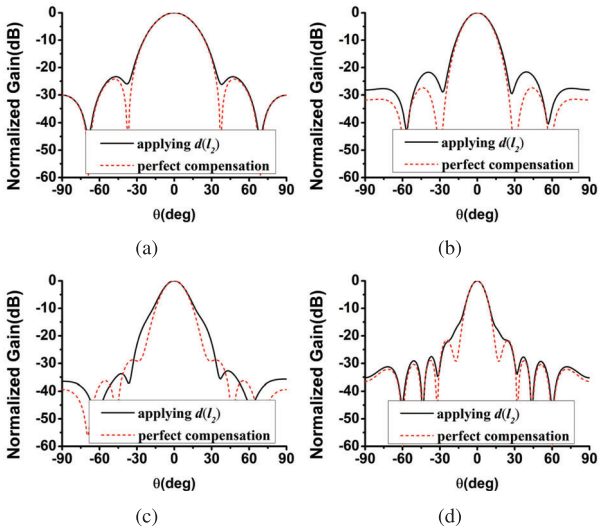

Fig. 8. Array factors from applying average curve $d(l_2)$ and perfect compensation for the X element at (a) 3, (b) 5, (c) 6, and (d) 8 GHz.

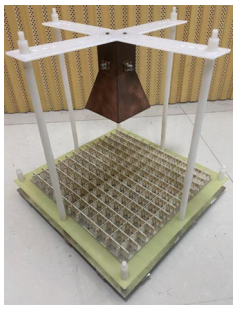

Fig. 9. Photograph of the tightly coupled dual-polarized reflectarray antenna.

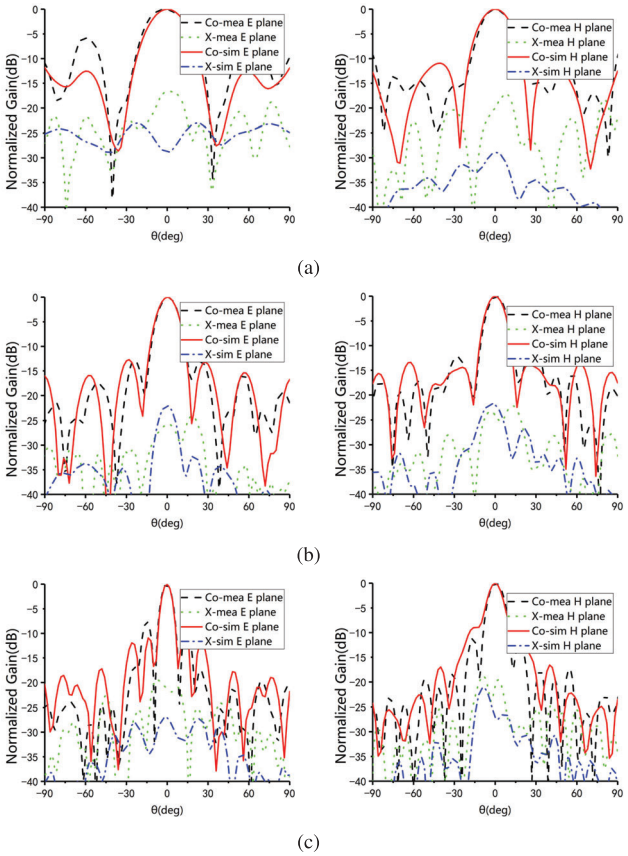

Fig. 10. X-polarization patterns of the reflectarray. (a)–(c) 3, 6, and 8 GHz.

all elements, which could be called perfect compensation. However, phase errors exist on the reflecting surface.

The phase error distribution of the X element is shown in Fig. 7. The max phase error of the X element is 90.5° and that of the Y element is 90°. The average phase error of the X element is 11.6°, 44.9°, 49.2°, and 36.9° at 3, 5, 6, and 8 GHz, respectively, and that of the Y element is 11.8°, 44.5°, 49.1°, and 36.9° at 3, 5, 6, and 8 GHz, respectively.

The phase error distribution has a strong influence on the radiation pattern of the reflectarray through the array factor. Fig. 8 shows the array factors from applying average curve $d(l_2)$ and perfect compensation for the X element. Employing the average curve degrades the patterns slightly. Relatively, the pattern at 6 GHz is impacted the most. The effects of the average curve on the Y element are similar to those of the X element. The array factors are stable despite the existence of the phase error, and the sidelobe level (SLL) is below −15 dB.

III. Prototype Development and Simulated and Measured Results

The proposed antenna is simulated in HFSS and measured in an anechoic chamber. The simulated and measured results of the antenna are shown in this section. The photograph of the antenna is shown in Fig. 9.

A. Radiation Patterns and Reflection Coefficient

The proposed antenna works in a large frequency range. The radiation patterns for the two polarizations are stable. The simulated and measured radiation patterns are shown in Figs. 10 and 11. The simulated results are in good agreement with the measured results. For most of X-polarization patterns, the highest SLL is below −10 dB, and the highest cross-polarization level is below −20 dB. For the most of Y-polarization patterns, the highest SLL is below −10 dB, and the highest cross-polarization level is below −22 dB.

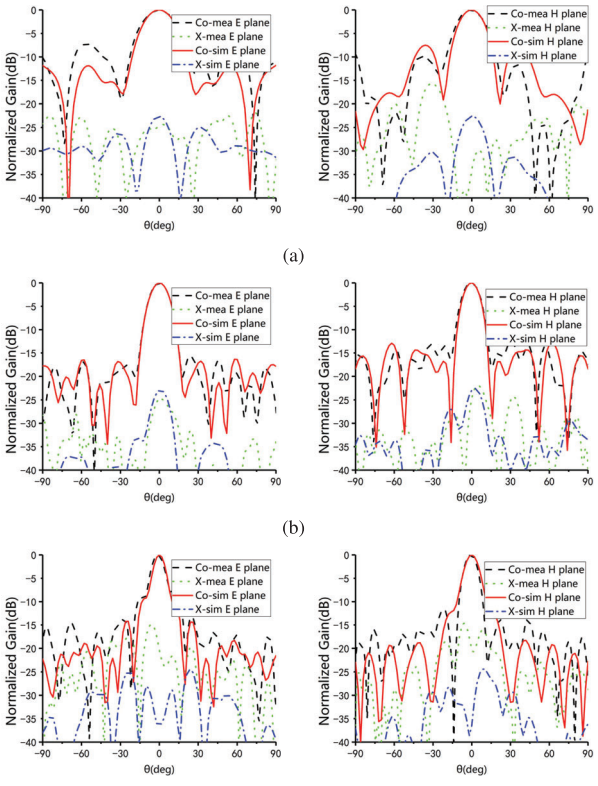

Fig. 11. Y-polarization patterns of the reflectarray. (a)–(c) 3, 6, and 8 GHz.

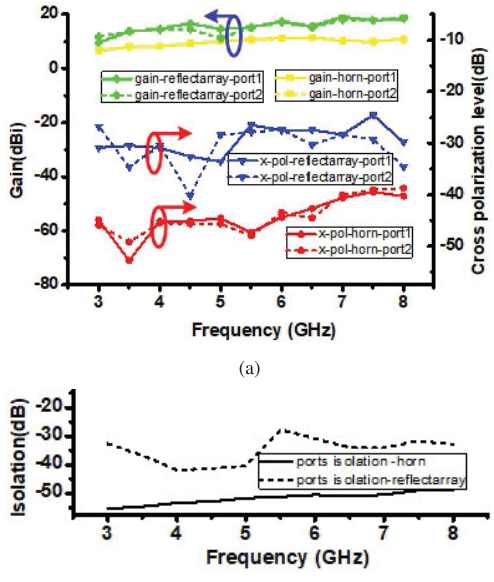

Fig. 12. (a) Gains, cross-polarization, and (b) isolation between the two ports of the feed antenna and the reflectarray.

There is no distortion in the shapes of the main beams for all the radiation patterns.

Fig. 12 shows the simulated isolation between the two ports, gains, and cross-polarization of the feed antenna and the reflectarray. Port 1 excites the X-polarized wave, while port 2 excites the Y-polarized wave. The gains of the reflectarray are higher than those of the horn antenna by about 10 dB. Compared with the horn antenna, the isolation and cross-polarization of the reflectarray degrade. The main beam directions of the X- and Y-polarized waves are the same, which means the cross-polarization wave is also strengthened in the main beam direction. So, the cross-polarization levels of the reflectarray degrade compared with that of the horn antenna. At the same time, the error of measurement could also lead to the measured cross-polarization levels being higher than the simulated results.

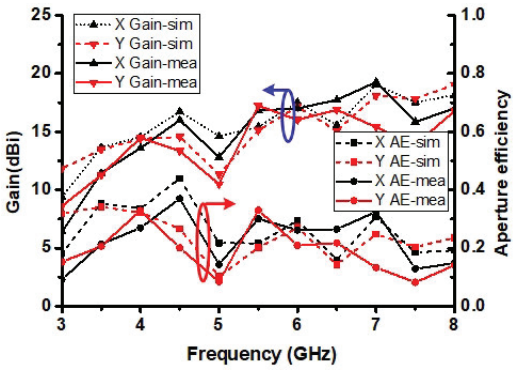

Fig. 13. Simulated and measured gains and AE.

TABLE IV
COMPARISON WITH WIDEBAND DUAL-POLARIZED REFLECTARRAYS IN REFERENCES

Ref. No.	Working bandwidth	Max aperture effi-ciency	Unit cell to achieve wide bandwidth
[5]	$\leq$ 1.38:1	77%	coplanar parallel dipoles
[12]	$\leq$ 1.38:1	37.4%	stacked dipoles
[13]	$\leq$ 1.54:1	20%	reconfigurable unit cell
[14]	$\leq$ 1.22:1	not given	stacked Jerusalem crosses
This paper	2.67:1	38.9%	tightly coupled element

B. Gain and Aperture Efficiency (AE)

In Fig. 13, the gains and AE are shown for both polarizations. For X-polarization, the simulated gain varies from 9.4 to 19.1 dBi, and the simulated AE varies from 18.1% to 43.9%. The measured gain varies from 6.4 to 19.1 dBi, and the measured AE varies from 15.1% to 38.9%. For Y-polarization, the simulated gain varies from 11.8 to 19.0 dBi, and the simulated AE varies from 14.3% to 34.1%. The measured gain varies from 9.3 to 17.5 dBi, and the measured AE varies from 12.1% to 31.8%.

Some wideband dual-polarized reflectarrays reported in the literature and the proposed reflectarray in this communication are compared in Table IV.

IV. CONCLUSION

A novel wideband dual-polarized reflectarray antenna based on tightly coupled dual-polarized unit cells is proposed. For both polarizations, the antenna has stable radiation patterns within the working band from 3 to 8 GHz. Over the entire working band, the antenna maintains stable main beams without distortion. In addition, the highest SLL of the radiation patterns can be maintained below −10 dB at most frequencies. The proposed reflectarray antenna is promising for applications that need antennas with wide bandwidth and dual polarizations.

REFERENCES

[1] R. D. Javor, X.-D. Wu, and K. Chang, "Design and performance of a microstrip reflectarray antenna," *IEEE Trans. Antennas Propag.*, vol. 43, no. 9, pp. 932–939, Sep. 1995.

[2] Y. Chen, L. Chen, H. Wang, X.-T. Gu, and X.-W. Shi, "Dual-band crossed-dipole reflectarray with dual-band frequency selective surface," *IEEE Antennas Wireless Propag. Lett.*, vol. 12, pp. 1157–1160, 2013.

[3] D. M. Pozar, S. D. Targonski, and H. D. Syrigos, "Design of millimeter wave microstrip reflectarrays," *IEEE Trans. Antennas Propag.*, vol. 45, no. 2, pp. 287–296, Feb. 1997.

[4] J. H. Yoon, Y. J. Yoon, W. S. Lee, and J. H. So, "Broadband microstrip reflectarray with five parallel dipole elements," *IEEE Antennas Wireless Propag. Lett.*, vol. 14, pp. 1109–1112, 2015.

[5] R. Florencio, J. A. Encinar, R. R. Boix, V. Losada, and G. Toso, "Reflectarray antennas for dual polarization and broadband telecom satellite applications," *IEEE Trans. Antennas Propag.*, vol. 63, no. 4, pp. 1234–1246, Apr. 2015.

[6] S. M. A. M. H. Abadi, K. Ghaemi, and N. Behdad, "Ultra-wideband, true-time-delay reflectarray antennas using ground-plane-backed, miniaturized-element frequency selective surfaces," *IEEE Trans. Antennas Propag.*, vol. 63, no. 2, pp. 534–542, Feb. 2015.

[7] P.-Y. Qin, Y. J. Guo, and A. R. Weily, "Broadband reflectarray antenna using subwavelength elements based on double square meander-line rings," *IEEE Trans. Antennas Propag.*, vol. 64, no. 1, pp. 378–383, Jan. 2016.

[8] W. Li, S. Gao, L. Zhang, Q. Luo, and Y. Cai, "An ultra-wide-band tightly coupled dipole reflectarray antenna," *IEEE Trans. Antennas Propag.*, vol. 66, no. 2, pp. 533–540, Feb. 2018.

[9] W. Li, "Design of printed array antennas for wireless communications," Ph.D. thesis, School Eng. Digit. Arts, Univ. Kent, Canterbury, U.K., 2018.

[10] J. Wang, Y. Zhou, and X. Feng, "A dual-polarized wideband tightly coupled reflectarray antenna proposed for 5G communication," in *Proc. Comput., Commun. IoT Appl. (ComComAp)*, Oct. 2019, pp. 200–203.

[11] L. Zhang et al., "A single-layer 10–30 GHz reflectarray antenna for the Internet of Vehicles," *IEEE Trans. Veh. Technol.*, vol. 71, no. 2, pp. 1480–1490, Feb. 2022.

[12] L.-X. Wu et al., "Wideband dual-feed dual-polarized reflectarray antenna using anisotropic metasurface," *IEEE Antennas Wireless Propag. Lett.*, vol. 21, no. 1, pp. 129–133, Jan. 2022.

[13] J. Yin, Q. Lou, H. Wang, Z. N. Chen, and W. Hong, "Broadband dual-polarized single-layer reflectarray antenna with independently controllable 1-bit dual beams," *IEEE Trans. Antennas Propag.*, vol. 69, no. 6, pp. 3294–3302, 2021.

[14] C. S. Geaney, M. Hosseini, and S. V. Hum, "Reflectarray antennas for independent dual linear and circular polarization control," *IEEE Trans. Antennas Propag.*, vol. 67, no. 9, pp. 5908–5918, Sep. 2019.

[15] Y.-M. Cai et al., "A novel ultrawideband transmitarray design using tightly coupled dipole elements," *IEEE Trans. Antennas Propag.*, vol. 67, no. 1, pp. 242–250, Jan. 2019.